

1 Polygenic Transcriptome Risk Scores 2 Can Translate Genetic Results 3 Between Species

4 **Natasha Santhanam^{1†}, Sandra Sanchez-Roige^{2,3†}, Yanyu Liang¹,**
5 **Apurva S. Chitre³, Daniel Munro^{3,5}, Denghui Chen³, Riyan Cheng³,**
6 **Jianjun Gao³, Anthony M. George⁷, Alex Gileta³, Katie Holl¹¹, Alesa**
7 **Hughson¹⁰, Christopher P. King⁶, Alexander C. Lamparelli¹⁴, Connor**
8 **D. Martin⁷, Angel Garcia Martinez⁹, Sabrina Mi¹, Celine L. St. Pierre³,**
9 **Jordan Tripi⁶, Tengfei Wang⁹, Hao Chen⁹, Shelly Flagel¹⁰, Keita**
10 **Ishiwari^{7,8}, Paul Meyer⁶, Laura Saba¹², Leah C. Solberg Woods¹³,**
11 **Oksana Polesskaya³, Abraham A. Palmer^{3,4*}, Hae Kyung Im^{1*}**

*For correspondence:

aap@ucsd.edu (AAP);

haky@uchicago.edu (HKI)

†These authors
contributed equally to this
work

Present address:

⁵Department of Psychiatry,
University of California San
Diego, La Jolla, CA, USA;

[¶]Genetic Medicine,
University of Chicago, US

12 ¹Department of Medicine, Section of Genetic Medicine, The University of
13 Chicago, Chicago, IL, 60637, USA; ²Department of Medicine, Division of
14 Genetic Medicine, Vanderbilt University Medical Center, Nashville, TN,
15 USA; ³Department of Psychiatry, University of California San Diego, La
16 Jolla, CA, 92093, USA; ⁴Institute for Genomic Medicine, University of
17 California San Diego, La Jolla, CA, 92093, USA; ⁵Department of Integrative
18 Structural and Computational Biology, Scripps Research, La Jolla, CA;
19 ⁶University at Buffalo, Department of Psychology, Buffalo, NY, 14260,
20 USA; ⁷University at Buffalo, Clinical and Research Institute on Addictions
21 University at Buffalo, Buffalo, NY, 14203, USA; ⁸University at Buffalo,
22 Pharmacology and Toxicology University at Buffalo, Buffalo, NY, 14203,
23 USA; ⁹University of Tennessee Health Science Center, Department of
24 Pharmacology, Addiction Science and Toxicology, Memphis, TN, 38163,
25 USA; ¹⁰University of Michigan, Department of Psychiatry, Ann Arbor, MI,
26 48109, USA; ¹¹Medical College of Wisconsin, Department of Pediatrics,
27 Milwaukee, WI, 53226, USA; ¹²University of Colorado Anschutz Medical
28 Campus, Department of Pharmaceutical Sciences, Aurora, CO 80045,
29 USA; ¹³Wake Forest University School of Medicine, Department of
30 Internal Medicine, Winston-Salem, NC, 27157, USA; ¹⁴Department of
31 psychology, University of California Los Angeles, Los Angeles, CA, 90095,
32 USA

34 **Abstract** Genome-wide association studies have demonstrated that most

35 traits are highly polygenic; however, translating these polygenic signals into
36 biological insights remains difficult. A lack of satisfactory methods for
37 translating polygenic results across species has precluded the use of model
38 organisms to address this problem. Here we explore the use of polygenic
39 transcriptomic risk scores (PTRS) for translating polygenic results across species.
40 Unlike polygenic risk scores (PRS), which rely on SNPs, PTRS use imputed gene
41 expression for prediction, which allows cross-species translation to orthologous
42 genes. We first developed RatXcan, which is a framework for
43 transcriptome-wide association studies (TWAS) in outbred rats. Leveraging
44 predicted transcriptome and genotype data from UK Biobank, and the
45 genetically trained gene expression models from RatXcan, we scored more than
46 3,000 rats using human-derived PTRS for height and BMI. Strikingly, we found
47 that these human-derived PTRS significantly predicted analogous traits in rats
48 ($r = 0.08$, $P = 8.57 \times 10^{-6}$; $r = 0.06$, $P = 8.51 \times 10^{-4}$, respectively). The genes
49 included in the PTRS were enriched for biological pathways including skeletal
50 growth and metabolism and were over-represented in tissues including
51 pancreas and brain. This approach facilitates experimental studies in model
52 organisms that examine the polygenic basis of human complex traits and
53 provides an empirical metric by which to evaluate the suitability of specific
54 animal models and identify their shared biological underpinnings.

55

56 Introduction

57 Over the last decade, genome-wide association studies (GWAS) have identified
58 numerous genetic loci that contribute to biomedically important traits [*Visscher*
59 *et al., 2017*]. However, translating these results into biologically meaningful dis-
60 coveries remains extremely challenging [*Lewis and Vassos, 2020, Martin et al.,*
61 *2019, Alliance et al., 2021*]. GWAS have demonstrated that most traits have a
62 highly polygenic architecture, meaning that numerous genetic variants with indi-
63 vidualy small effects confer risk [*Loos, 2020*]. The cumulative results from GWAS
64 can be used to construct polygenic risk scores (PRS), which summarize the effects
65 of many loci on a trait [*Wray et al., 2007*].

66 Model organisms provide a system in which the effect of genotype, genetic
67 manipulations and environmental exposures can be experimentally tested. Whereas
68 the tools for using model organisms to study *individual* genes are well established,
69 there are no satisfactory methods for studying the *polygenic* signals obtained
70 from GWAS in model organisms. PRS are not suitable because they summarize
71 the effects of many single-nucleotide polymorphisms (SNPs) on a trait; however,
72 humans SNPs do not have direct homologs in other species, and even if they did,
73 they would not be expected to have the same effects or to tag the same causal
74 variants.

75 To address this problem, we sought to develop a novel method that allows
76 translation of polygenic signals from humans to other species and vice-versa.
77 This method focuses on gene expression, rather than SNPs, and builds on our
78 past work with polygenic transcriptomic risk scores (PTRS) [*Liang et al., 2022*].
79 PTRS are premised on the regulatory nature of most GWAS loci [*Maurano et al.,*
80 *2012*] and use genetically regulated gene expression (transcript abundance), in-
81 stead of SNPs as features for prediction. We recently showed that PTRS are useful
82 for translating polygenic signals between different human ancestry groups [*Liang*
83 *et al., 2022*], supporting the view that the effects of genes on a phenotype are con-
84 served across ancestry groups. In the current project we hypothesized that the
85 relationships between genes and phenotypes are conserved not only between
86 human ancestry groups, but also across species. Thus, we explored whether
87 PTRS trained using human data could predict similar traits in another species
88 by applying the PTRS to orthologous genes in the target species. We selected
89 heterogeneous stock (HS) rats because they are a well characterized, outbred
90 mammalian population for which dense genotype, phenotype and gene expres-
91 sion data are available in thousands of subjects [*Solberg Woods and Palmer,*
92 *2019*] [*Chitre et al., 2020*].

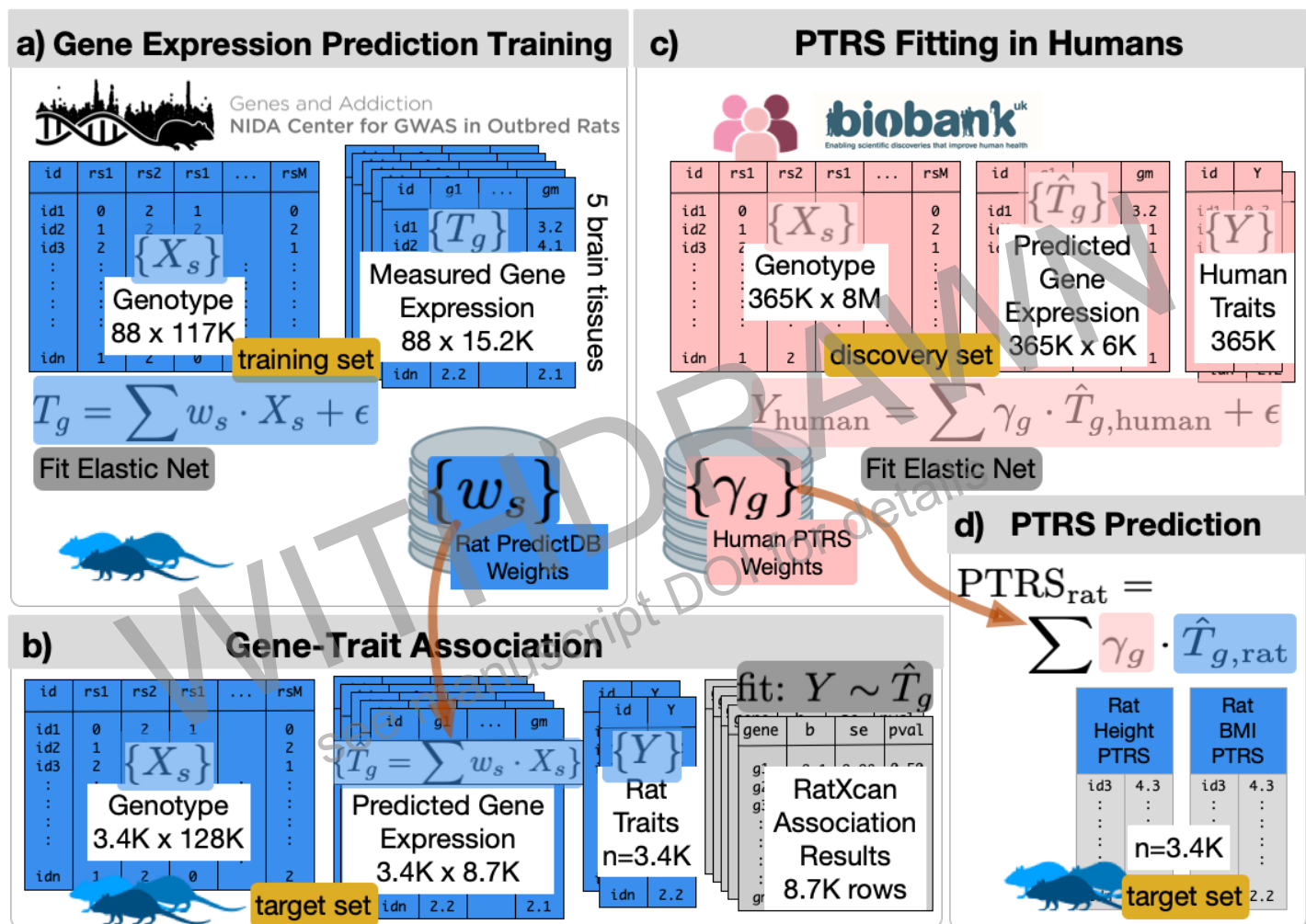


Figure 1. Schematic representation of cross-species polygenic translation framework.

The workflow was divided into 4 stages: a) gene expression prediction training, b) gene-trait association, c) PTRS fitting in humans, d) PTRS prediction. a) In the gene expression prediction training stage, we used genotype (117,155 SNPs) and gene expression data (15,216 genes) from samples derived from 5 brain regions in 88 rats. The prediction weights (rat PredictDB weights) are stored in predictdb.org. Rats used in this stage constitute the training set. b) In the gene-trait association stage, we used genotype and phenotype data from the target set of 3,407 rats (no overlap with training set rats). Predicted gene expression (8,567 genes for which prediction was possible) was calculated for all the 3,407 target set rats, and gene-trait associations were tested using RatXcan (N=1,463-3,110). We queried human gene-level associations from PhenomeXcan to estimate enrichment levels with our rat findings. c) Human PTRS weights were fitted using elastic net regression of height and BMI on predicted whole blood gene expression levels (7,002 genes) in the UK Biobank (N=356,476). d) The human PTRS weights were used for complex trait prediction in rats. PTRS trained in humans were then used to predict analogous traits in our target rat set. Prediction performance of PTRS was calculated as the correlation (and partial correlation) between the predicted scores in rats and the observed traits. Analyses in rats are shown in blue and analyses in humans are shown in pink.

93 Results

94 Experimental setup

95 To build a framework for translating genetic results between species, we followed
96 the experimental setup illustrated in Fig. 1. In the *training stage* (Fig. 1a), we inves-
97 tigated the genetic architecture of gene expression and built prediction models
98 of gene expression in rats. We used genotype and transcriptome data from five
99 brain regions sampled from 88 rats, generated by the [NIDA Center for GWAS for](#)
100 [Outbred rats](#) (Fig. 1a). In the *association stage* (Fig. 1b), we used their genotype
101 data to predict the transcriptome in a non-overlapping *target set* of 3,407 rats and
102 tested for association between the genetically predicted gene expression and 7
103 physiological traits by adapting the PrediXcan software, which was originally de-
104 veloped for use in humans [[Gamazon et al., 2015](#)] to rats ('RatXcan'). The phys-
105 iological traits were: body length, body weight, BMI (body length/body weight²),
106 three fat pad weights, and fasting glucose. In the *discovery stage* (Fig. 1c), we de-
107 termined the human-derived PTRS weights for height and BMI using data from
108 356,476 individuals of European-descent from UK Biobank. In the final stage (Fig
109 1d), we used these human-derived weights in conjunction with genetically pre-
110 dicted gene expression for rats in the target set. We assessed the prediction per-
111 formance by comparing the predictions from the PTRS to the true body length
112 (which is equivalent to human height) and BMI for each rat.

113 Genetic Architecture of Gene Expression across Brain Tissues

114 To inform the optimal prediction model training, we examined the genetic archi-
115 tecture of gene expression by quantifying its heritability and polygenicity. Unless
116 otherwise specified, we show the results for nucleus accumbens core in the main
117 section and for the remaining tissues in the supplement.

118 We calculated the heritability of expression for each gene by estimating the
119 proportion of variance explained (PVE) using a Bayesian Sparse Linear Mixed
120 Model (BSLMM) [[Zhou et al., 2013](#)]. We restricted the feature set to variants within
121 1 Mb of the transcription start site of each gene since this is expected to capture
122 most cis-eQTLs. Among the 15,216 genes considered, 3,438 genes were heritable
123 in the nucleus accumbens core, with 95% credible sets's lower boundary greater
124 than 1%. The mean heritability ranged from 8.86% to 10.12% for all brain tissues
125 tested (Table 1). Fig. 2a shows the heritability estimates for gene expression
126 in the nucleus accumbens core, while heritability estimates in other tissues are
127 shown in Fig. S1. In humans, we identified a similar heritability distribution (Fig.
128 2b, Fig. S2) based on whole blood samples from GTEx.

129 Next, to evaluate the polygenicity of gene expression levels, we examined
130 whether predictors with more polygenic (i.e., many variants of small effects) or
131 more sparse (i.e., just a few larger effect variants) architecture correlated better

132 with observed expression. We fitted elastic net regression models using a range
133 of mixing parameters from 0 to 1 (Fig. 2c). The leftmost value of 0 corresponds
134 to ridge regression, which is fully polygenic and uses all cis-variants. Larger val-
135 ues of the mixing parameters yield more sparse predictors, with the number of
136 variants decreasing as the mixing parameter increases. The rightmost value of 1
137 corresponds to lasso, which yields the most sparse predictor within the elastic net
138 family. Similar to reports in human data [Wheeler et al., 2016], sparse predictors
139 outperformed polygenic predictors (Fig. 2c).

140 We used the 10-fold cross-validated Pearson correlation (R) between predicted
141 and observed values as a measure of performance (Spearman correlation yielded
142 similar results). We observed a substantial drop in performance towards the
143 more polygenic end of the mixing parameter spectrum (Fig. 2c). For reference,
144 we show similar results using human gene expression data from whole blood
145 samples in GTEx individuals (Fig. 2d). Overall, these results indicate that the ge-
146 netic architecture of gene expression in rats (detectable at current sample sizes)
147 is sparse, similar to that of humans [Wheeler et al., 2016].

148 **Generation of Prediction Models of Gene Expression in Rats**

149 Based on the relative performance across different elastic net mixing parameters,
150 we chose a value of 0.5, which yielded slightly less sparse predictors than lasso
151 but provided robustness to missing or low quality variants; this is the same value
152 that we have chosen in the past for humans datasets [Gamazon et al., 2015].

153 We trained elastic net predictors for all genes in all 5 brain regions. The proce-
154 dure yielded 8,244-8,856 genes across five brain tissues from the available 15,216
155 genes (Table 1). The 10-fold cross-validated prediction performance (R^2) ranged
156 up to 80% with a mean of 8.51% in the nucleus accumbens core. Similarly to Fig. 1a
157 and b, mean prediction R^2 was consistently lower than mean heritability, as is ex-
158 pected since genetic prediction performance is restricted by its heritability. Other
159 brain tissues yielded similar prediction performance (Table 1). Reassuringly, pre-
160 diction performance values followed the heritability curve, confirming that genes
161 with highly heritable expression tend to be better predicted than genes with low
162 heritability in both rats and humans (Fig. 2a-b). Interestingly, we identified better
163 prediction performance in rats than in humans (Fig. S3), despite heritability of
164 gene expression being similar across species (Fig. 2a-b).

165 In Fig. 3a-b, we show the prediction performance of two of the best predicted
166 genes in rats (*Mgmt*, $R^2 = 0.72$) and humans (*RPS26*, $R^2 = 0.74$). Across all genes,
167 we found that the prediction performance in rats was correlated with that of hu-
168 mans ($R = 0.061$, $P = 8.03 * 10^{-6}$; Fig. 3c). Furthermore, performance per gene be-
169 tween two tissues was similar in both rats (Fig. 3d) and humans (Fig. 3e), namely,
170 genes that were well-predicted in one tissue were also well-predicted in another
171 tissue. Correlation of prediction performance across tissues ranged from 58 to

172 84% in rats and 42 to 69% in humans.

173 Having established the similarity of the genetic architecture of gene expres-
174 sion between rats and humans, we transitioned to the *association stage*.

Brain Region	# Rats	# Genes Predicted	Average R^2	Average cis h^2
Nucleus Accumbens Core (NAcc)	78	8,567	8.51%	9.82%
Infralimbic Cortex (IL)	83	8,856	8.87%	9.77%
Lateral Habenula (LHb)	83	8,244	7.78%	8.86%
Prelimbic Cortex (PL)	81	8,315	9.33%	10.12%
Orbitofrontal Cortex (OFC)	82	8,821	9.13%	9.82%

Table 1. Summary of heritability and prediction performance in rats. The table shows the number of rats used in the prediction, number of genes predicted per model, the average prediction performance R^2 , and average cis-heritability cis h^2 , for all gene transcripts.

175 **PrediXcan/TWAS Implementation in Rats (RatXcan)**

176 To extend the PrediXcan/TWAS framework to rats, we developed RatXcan. We
177 used the predicted weights from the *training stage* to estimate the genetically reg-
178 ulated expression in the *target set* of 3,407 rats. We then tested the association
179 between predicted expression and seven physiological traits.

180 We identified 90 Bonferroni significant genes ($P(0.05/5388) = 9.28 \times 10^{-6}$) in
181 57 distinct loci separated by ± 1 MB for rat body length (Fig. 4a) and 21 signifi-
182 cant genes in 15 loci for rat BMI (Fig. 4b; Supplementary Table 1). Among the
183 top significant genes, *Adcy3* was associated with fat traits ($P = 7.22 \times 10^{-16}$) and
184 body weight ($P = 2.41 \times 10^{-4}$). The human ortholog, *ADCY3*, was associated with
185 BMI [*Speliotes et al., 2010*] and was reported to mediate energy homeostasis
186 and is considered a promising therapeutic target for obesity [*Saeed et al., 2018*].
187 Similarly, *Prhr* was associated with fat traits, body weight, BMI, and body length
188 ($P = 5.55 \times 10^{-17}$, $P = 2.81 \times 10^{-16}$, $P = 5.12 \times 10^{-12}$, $P = 4.65 \times 10^{-04}$, respectively).
189 The human ortholog, *PRLHR*, was associated with BMI and body fat percentage
190 ($P = 1.76 \times 10^{-6}$, $P = 3.62 \times 10^{-6}$) [*Pividori et al., 2020*]. *PRLHR* encodes for a 7-
191 transmembrane domain receptor for prolactin-releasing hormone [*Ozawa et al.,*
192 **2002**]. *PRLHR* was found to be associated with lactation, regulation of food intake
193 and pain-signal processing [*Atanes et al., 2021*]. Moreover, both *Adcy3* and *Prhr*
194 have previously been identified as candidate genes for adiposity in the HS rat
195 population [*Chitre et al., 2020*].

196 To evaluate whether trait-associated genes in rats were more significantly
197 associated with the corresponding trait in humans, we performed enrichment
198 analysis. Specifically, we selected genes that were nominally associated with rat

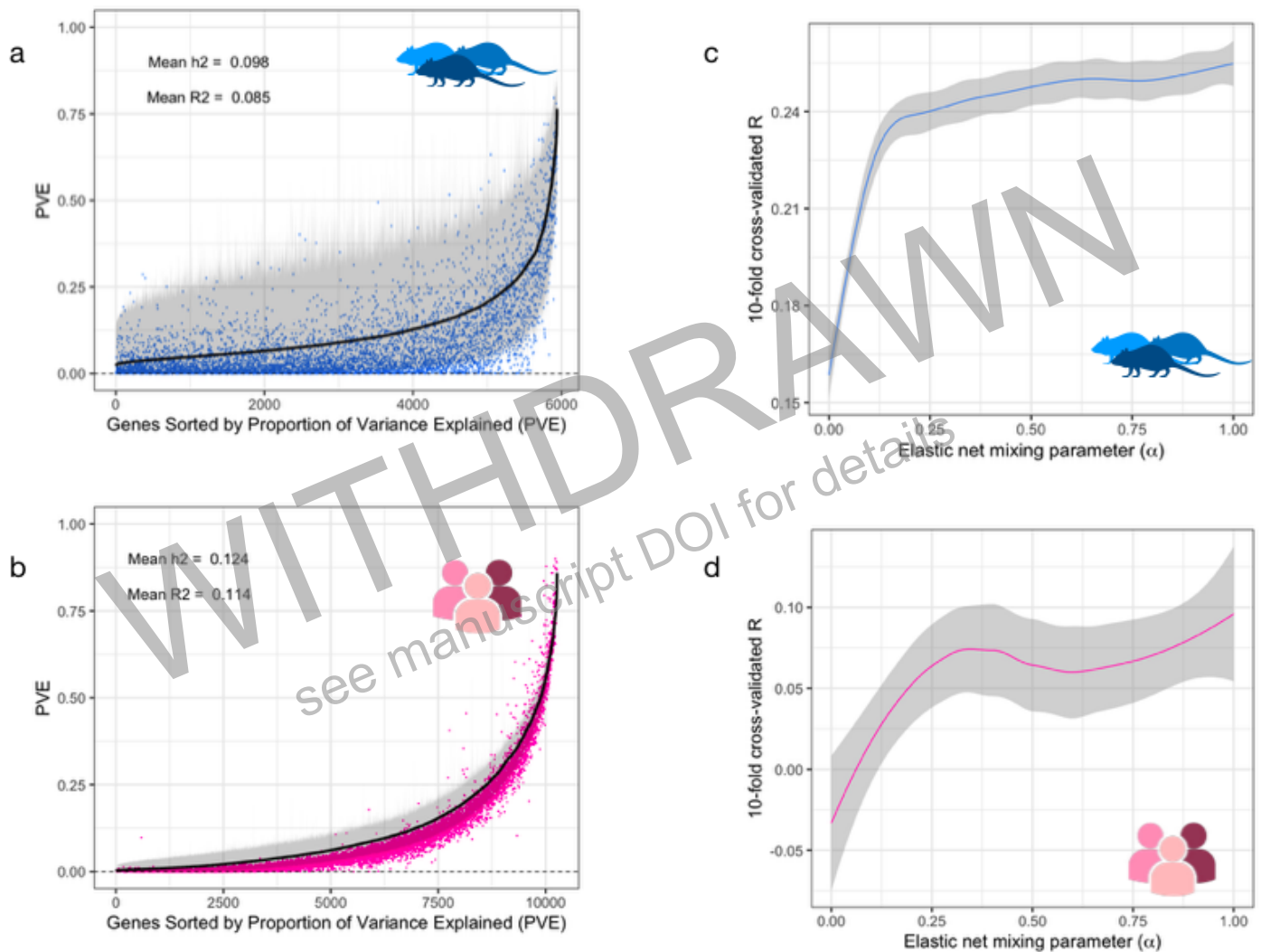


Figure 2. Heritability and sparsity of gene expression in both rats and humans. a) cis-heritability of gene expression levels in the nucleus accumbens core of rats calculated using BSLMM (black). We show only genes ($N = 10,268$) that have an equivalent ortholog in the GTEx population. On the x-axis, genes are ordered by their heritability estimates. 95% credible sets are shown in gray for each gene. Blue dots indicate the prediction performance (cross validated R^2 between predicted and observed expression). b) cis heritability of gene expression levels in whole blood tissue in humans from GTEx. We show only the same 10,268 orthologous genes. On the x-axis, genes are ordered by their heritability estimates. 95% credible sets are shown in gray for each gene. Pink dots indicate the prediction performance (cross validated R^2 between predicted and observed expression). c) Cross validated prediction performance in rats (Pearson correlation R) as a function of the elastic net parameter ranging from 0 to 1. d) Cross validated prediction performance in humans (Pearson correlation R) as a function of the elastic net parameter ranging from 0 to 1.

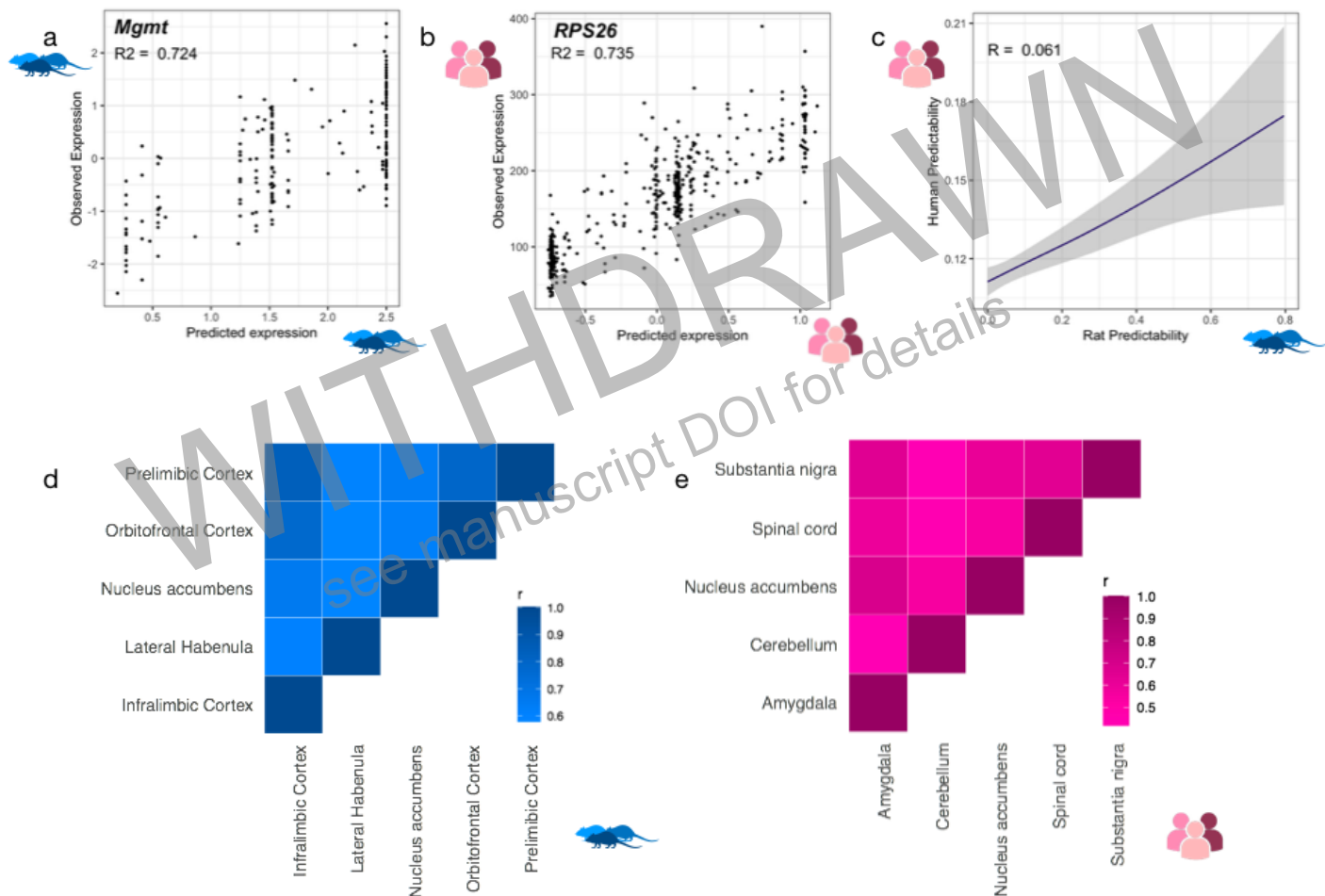


Figure 3. Shared genetic architecture of gene expression in rats and humans a) Comparison of predicted vs. observed expression for a well predicted gene in rats (*Mgmt*, $R^2 = 0.72$, $R = 0.65$, $P < 2.20 \times 10^{-16}$). b) In humans, predicted and observed expression for *RPS26* were significantly correlated ($R^2 = 0.74$, $R = 0.86$, $P < 2.20 \times 10^{-16}$). c) Prediction performance was significantly correlated across species ($R = 0.06$, $P = 8.03 \times 10^{-06}$) d-e) and across all five brain tissues tested in rats and humans. In rats, within tissue prediction performance ranged from ($R = [0.58 - 0.84]$, $P < 2.20 \times 10^{-16}$). In humans, the range was [$R = 0.42 - 0.69$, $P < 2.20 \times 10^{-16}$].

199 body length ($P < 0.05$) and compared the p-value from the analogous human
200 trait (height) against the background distribution. Given the large sample size of
201 human height GWAS, we expected the background distribution (shown in pink,
202 Fig. 4c) of height gene-based associated p-values to depart substantially from
203 the identity line (in gray). The subset of genes that were associated with rat body
204 length (in blue, Fig. 4c) showed a major departure from the background distribu-
205 tion, indicating that body length genes in rats were more significantly associated
206 with human height than expected. To quantify the enrichment, we compared the
207 p-value distribution of all the genes with the distribution of the subset of genes
208 that were nominally significantly associated with rat body length ($P = 6.55 \times 10^{-10}$).
209 Similar enrichment was found for BMI (Fig. 4d) ($P = 8.07 \times 10^{-07}$). This systematic
210 enrichment across human and rat findings further encouraged us to test whether
211 PTRS based on human studies could predict analogous traits in rats.

212 **Transfer PTRS from Humans to Rats**

213 To test the portability of PTRS across species, we started by calculating the hu-
214 man PTRS weights, as described in *Liang et al. [2022]*. Using 356,476 UK Biobank
215 unrelated European descent individuals, we fitted an elastic net regression with
216 height as the outcome variable and the imputed gene expression as the predictor
217 ($\text{height} = \sum_g \gamma_g \cdot T_g + \epsilon$ with ϵ , an error term and T_g the imputed gene expression in
218 humans). We chose to use GTEx whole blood predictors, as it was previously re-
219 ported to perform well in humans [*Liang et al., 2022*]. We applied this procedure
220 for a range of elastic net regularization parameters to increase the flexibility of
221 the prediction models, resulting in 37 sets of weights. The regularization param-
222 eter is a hyper-parameter that can be estimated in a validation set, which could
223 be a subset of the target set. Here we show the prediction performance across
224 the full range of hyper-parameters (37 models).

225 For each rat in the target set, we calculated 37 PTRS (one for each regulariza-
226 tion parameter) as the weighted sum of the predicted gene expression in rats
227 with the human-derived weights, which were already computed during the asso-
228 ciation stage ($\text{PTRS}_{\text{rat}} = \sum_g \gamma_g \cdot T_{g,\text{rat}}$). We used a range of 1 to 2,017 genes, after
229 limiting the human genes that had orthologs in rats (28.72%), to discern how pre-
230 diction varied as the number of genes changed. The large number of genes used
231 for prediction is consistent with prior human literature indicating that the genetic
232 architecture of height consists of a large number of genes [*Wood et al., 2014*].

233 Consistent with prior human literature [*Yengo et al., 2018*] [*Zhao et al., 2015*],
234 gene set enrichment analyses showed that the genes used to calculate human
235 PTRS weights were substantially enriched for pathways and tissues that contribute
236 to skeletal growth and metabolic processes, including myogenesis ($P = 1.18 \times$
237 10^{-5}), adipogenesis ($P = 7.74 \times 10^{-17}$) and fatty acid metabolism ($P = 3.97 \times 10^{-15}$)
238 (ST. 16). Tissue analysis revealed that PTRS genes are enriched as differentially ex-

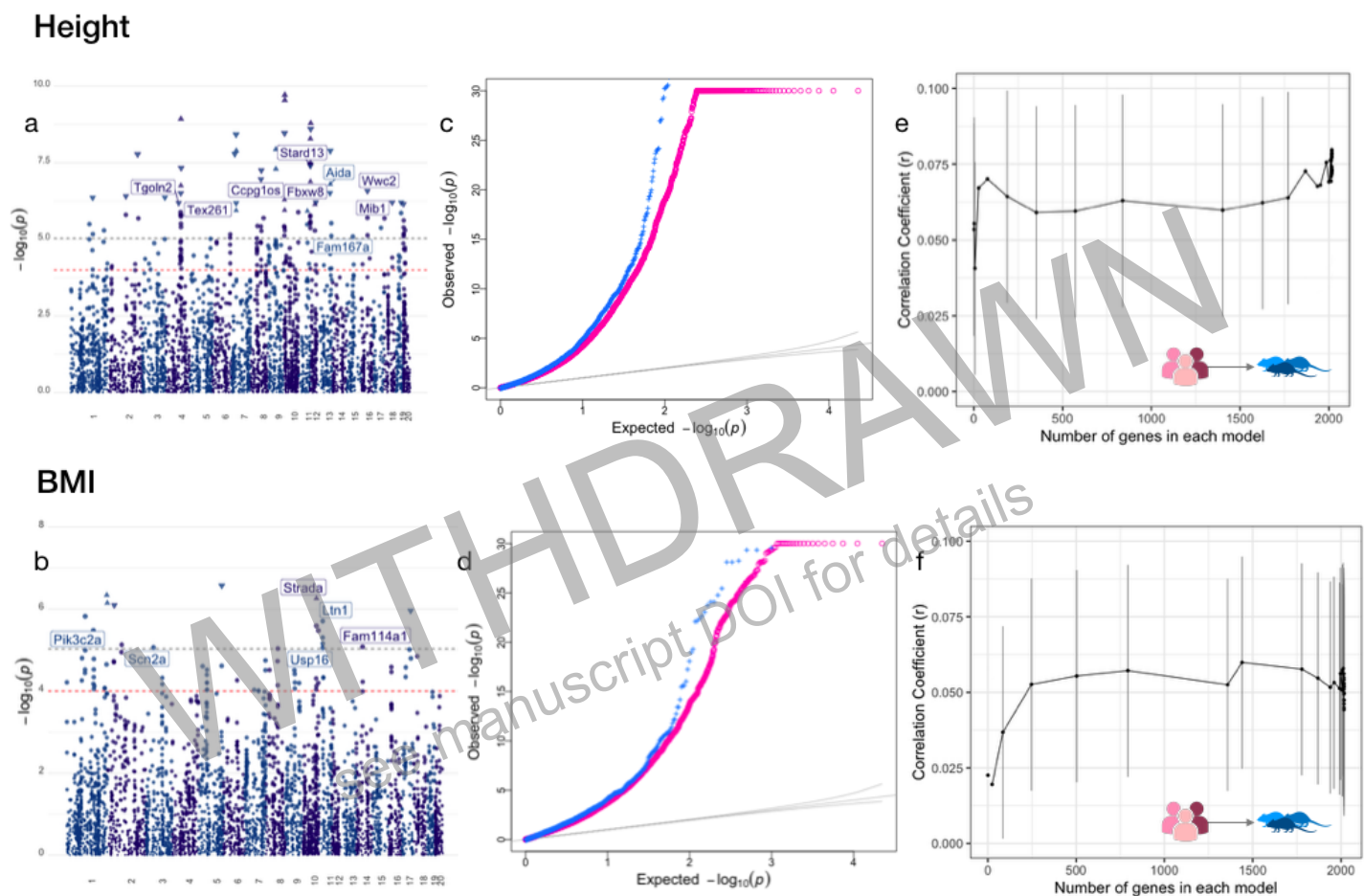


Figure 4. Polygenic Transcriptomic Risk Scores (PTRS) can translate genetic information across species. a) Manhattan plot of the association between predicted gene expression and rat body length, which is analogous to human height. b) Manhattan plot of the association between predicted gene expression and rat BMI. In both a) and b) we label the genes whose human orthologs are at least nominally associated in human data ($P < 0.01$); Grey dotted line corresponds to the Bonferroni correction threshold of $0.05/5,388$ of tests. Red dotted line corresponds to an arbitrary threshold of 1×10^{-4} . Triangular points refer to genes that were significantly associated with body length at the Bonferroni threshold, where the direction of the triangle corresponds with the sign of the associated gene. c) Q-q plot of the p-values of the association between predicted gene expression levels in humans (phenomexcan.org). Pink dots correspond to all genes tested in humans. Blue dots correspond to the subset of genes that were nominally significantly associated with body length in rats ($P < 0.05$). d) Q-q plot of the p-values of the association between predicted gene expression levels in humans (phenomexcan.org). Pink dots corresponds to all genes in humans. Blue dots correspond to the subset of genes that were nominally significantly associated with BMI in rats ($P < 0.05$). e) Correlation between human-derived height PTRS and observed body length in rats for the 37 regularization parameters used in building the PTRS. f) Correlation between human-derived BMI PTRS and observed BMI in rats for the 37 regularization parameters used in building the PTRS. (The confidence intervals for models 1 and 2 include zero, not shown.)

239 pressed genes in multiple relevant tissues, including pancreas, heart, liver, and
240 central nervous system (Fig. S4).

241 Strikingly, human-derived height PTRS significantly predicted body length in
242 rats; that is, the correlation between PTRS and observed rat body length was sig-
243 nificant for all the elastic net regularization parameters that included at least 27
244 genes (maximum $R = 0.08$, $P = 8.57 \times 10^{-6}$; Fig. 4e). To compare our prediction
245 performance to that in the human population, we used the partial R^2 (\tilde{R}^2 , the
246 proportion of variance explained by the predictor after accounting for other co-
247 variates) reported by *Liang et al. [2022]*. The partial \tilde{R}^2 for body length in rats was
248 0.64% ($P = 8.57 \times 10^{-6}$), while in the UK Biobank European test set, the partial \tilde{R}^2
249 for height in humans was 9.40%.

250 We applied the same procedure to BMI and again found significant predic-
251 tion; the correlation between human-derived BMI PTRS and observed BMI was
252 significant across all regularization parameters that included at least 247 genes
253 (maximum $R = 0.06$, $P = 8.51 \times 10^{-4}$; Fig. 4f). The maximum partial \tilde{R}^2 was 0.36%
254 ($P = 8.52 \times 10^{-4}$). In UK Biobank European test set, the partial \tilde{R}^2 for BMI in humans
255 was 1.45%.

256 As a negative control, we compared the correlation between the human-derived
257 height PTRS and observed fasting glucose in the target set of rats. As shown in Fig.
258 S5, the correlation was not significant ($P = 0.71$), confirming that a human-derived
259 PTRS can predict a similar trait in rats, but do not predict dissimilar traits.

260 Discussion

261 Overwhelming evidence demonstrates that most complex diseases are extremely
262 polygenic, however there are no methods for translating polygenic results in
263 other species. Here, we present a novel analytical framework that facilitates
264 cross-species translation of polygenic results, providing a unique and urgently
265 needed bridge between the human and model organism disciplines. Translation
266 of polygenic information has been challenging because, despite the utility of PRS
267 for trait prediction in humans, SNPs do not transfer across species. Our approach
268 circumvents this limitation by translating polygenic information to the level of
269 genes and then relying on the mapping of orthologous genes between humans
270 and another species, in this case rats.

271 A critical first step in this project was the development of RatXcan, which is
272 the rat version of PrediXcan [*Gamazon et al., 2015*], which is a well-established
273 statistical tool that is used in human genetics. We showed that the genetic archi-
274 tecture of gene expression in rats is broadly similar to humans: they are heritable,
275 sparse, and the degree of heritability is preserved across tissues; some of these
276 observations are consistent with another recent publication that mapped eQTLs
277 in HS rats [*Munro et al., 2022*]. Interestingly, despite the smaller sample sizes

278 used to train our prediction models, rats showed better prediction than humans.
279 This might reflect the fact that HS rats have a preponderance of common alleles
280 [Chitre *et al.*, 2020] whereas humans have numerous rare alleles that influence
281 gene expression but are difficult to capture in prediction models. The superior
282 prediction may also reflect the longer haplotype blocks that are present in HS
283 rats relative to humans [Chitre *et al.*, 2020].

284 Using RatXcan, we tested gene-level associations of 7 physiological traits that
285 had been previously measured in rats. Our main focus was on height and BMI
286 because of the availability of large human GWAS that allowed us to develop ro-
287 bust human PTRS for those traits and because of the relatively unambiguous sim-
288 ilarity between traits in humans and rats. We found substantial enrichment of
289 trait-associated genes among orthologous human trait-associated genes, which
290 encouraged us to use the human PTRS to try to predict similar traits in the HS
291 rats.

292 Remarkably, we found that PTRS developed in humans significantly predicted
293 both rat body length (which is equivalent to height) and BMI in rats. These re-
294 sults demonstrate that PTRS is a viable strategy for translating polygenic results
295 between humans and rats. Even though, the proportion of body length variance
296 explained by our PTRS was only 0.64% compared to the 9.40% in the European
297 target set, that proportion dropped substantially as low as 1.46% when testing
298 in non European target sets (See supplementary Table 6 in [Liang *et al.*, 2022]).
299 Closer examination of these results revealed that prediction of height improved
300 until about 100 genes were included in the model, whereas prediction of BMI con-
301 tinued to improve until about 250 genes were included in the model. It is likely
302 that larger and thus more powerful rat transcriptomic datasets would improve
303 prediction by increasing the number of genes that contributed to prediction as
304 well as the accuracy of prediction. In addition, of the 7,044 genes that were in-
305 cluded in the human-derived PTRS, only 2,017 had rat orthologs; increasing our
306 knowledge of orthologous genes or identifying other strategies to address this
307 limitation might further improve performance.

308 The magnitude and significance of prediction using human PTRS for BMI to
309 predict rat BMI was smaller than it was for human height to rat body length, which
310 was expected given the lower heritability of human BMI. For reference, heritabil-
311 ity estimates were more than three-fold lower for human BMI as compared to
312 human height: 15% for BMI vs. 55% for height [Liang *et al.*, 2022]. The ability
313 to transfer polygenic signals to other species creates novel opportunities to ex-
314 plore the mechanisms underlying those traits. For example, genes included in the
315 human-derived PTRS showed evidence of enrichment in relevant pathways and
316 tissues for skeletal and metabolic processes, demonstrating that PTRS can un-
317 cover shared underlying biological mechanisms, which can be more intensively
318 studied in model systems. It is also possible that PTRS could be used to iden-

319 tify which aspects (e.g. tissues, cell types, etc) of a human trait are recapitu-
320 lated by analogous phenotypes in model organism, which could highlight both
321 the strengths and limitations of a phenotype that is used to model a disease or
322 other human trait.

323 For example, PTRS will provide a novel means of validating animal models of
324 human disorders, as it will be possible to empirically test whether the genetic
325 signature for a particular condition in humans is related to that of analogous
326 phenotypes in rodents. Notably, PTRS captures both the magnitude and the di-
327 rectionality of each gene's effect on a phenotype. A potential application of PTRS
328 could be to categorize rodents as being more or less susceptible to human traits
329 and diseases aimed at quantifying whether non-genetic parameters (e.g., drugs,
330 environmental stressors) alter gene expression in a way that modifies the PTRS.
331 Another advantage of our approach is that it focuses on the role of several genes
332 involved in a phenotype. Thus, PTRS could also serve as a toolkit for identify-
333 ing components of molecular networks for drug repositioning, namely studies
334 aimed at identifying small molecules and other interventions that can alter the
335 global gene expression in model organisms in a way that lowers risk, as predicted
336 by PTRS analyses.

337 There is a widely recognized need for methods to integrate data from genetics
338 studies in humans and non-humans [*Palmer et al., 2021b*]. To address this need,
339 several prior efforts combine human genetic results with sets of genes identi-
340 fied as differential expressed in various model organisms [*Reynolds et al., 2021*].
341 Two such studies examined the overlap between human GWAS results for traits
342 related to human substance use disorder and changes in gene expression in the
343 brain, typically following acute or chronic administration of drugs. In two of these
344 approaches, gene sets were collected from rodent differential gene expression
345 studies that examined the effects of alcohol and/or nicotine and then used a parti-
346 tioned heritability approach, which showed enrichment of these genes in human
347 GWAS results [*Palmer et al., 2021a*], although there was some question about the
348 specificity of the effects [*Huggett et al., 2021*]. Another study used a broadly sim-
349 ilar approach but also included protein-protein network information [*Mignogna*
350 *et al., 2019*]. In yet another study that examined polygenicity in rodents, a cross
351 was made to introduce genetic variability among mice that all carried the 5XFAD
352 transgene, which recapitulates some features of Alzheimer's disease (AD). By clas-
353 sifying mice based on their genotype at 19 markers that were near genes impli-
354 cated by human GWAS for AD, they showed evidence of epistatic modulation of
355 the phenotypic effects of the 5XFAD allele by these 19 markers [*Neuner et al.,*
356 *2019*]. While this approach shares the most commonalities with PTRS, Neuner et
357 al [*Neuner et al., 2019*] did not extrapolate GWAS data to transcript abundance,
358 did not preserve the weights and directionality available from TWAS and account
359 for whether or not the mouse genes showed heritable gene expression differ-

360 ences.

361 Our studies are conceptually similar to studies that seek to examine cellular
362 and molecular phenotypes in cultured human cells for which PRS have been calcu-
363 lated [*Dobrindt et al., 2020*]. In a similar manner, rats or other model organisms
364 could be assigned PTRS such that rats with a high or low risk of a uniquely human
365 phenotype, such as schizophrenia, could be examined to identify molecular, cel-
366 lular or circuit level differences between rats with high or low scores. Similarly,
367 just as pharmacological manipulation can be applied to cells in culture that have
368 been sorted for PRS or PTRS scores [*So et al., 2017*], pharmacological treatments
369 could be administered to a model species to see if the gene expression pattern
370 changed in a manner associated with reduced risk for a disease or other condi-
371 tion.

372 There are several limitations in the current study that need be addressed in
373 the future. The sample size of the reference transcriptome data in rats was lim-
374 ited. We would expect better predictability estimates in our elastic-net trained
375 models with larger sample sizes. Second, presumably due to the lack of ade-
376 quate sample size, we did not have a sufficiently robust PTRS from rats to at-
377 tempt rat to human PTRS translation. Third, we suspect that in both humans and
378 rats, some gene-level associations may be confounded by linkage disequilibrium
379 contamination and co-regulation. This problem is likely to be more serious in
380 model organisms where even longer range LD exists. Refining PTRS by integrat-
381 ing fine-mapping and co-localization approaches could improve portability across
382 species. Finally, integration of other omic data types (e.g., protein, methylation,
383 metabolomics) and the use of cell-specific data may improve prediction accuracy
384 and cross-species portability. It is worth noting that while we have shown success
385 with humans and rats, it is still not clear whether more distantly related species,
386 such as non-mammalian vertebrates or even insects, might also lend themselves
387 to the PTRS approach.

388 Despite these limitations, we have shown that PTRS, which has previously
389 been used to address the difficulty of transferring PRS between human ancestries
390 [*Liang et al., 2022*], can successfully transfer polygenic results between species.
391 One important feature of this approach is its ability to preserve both magnitude
392 and directional information about the relationship between gene expression and
393 phenotype. This method should support new and transformative experimental
394 designs. Most importantly, it provides a method to empirically validate traits that
395 are studied in model systems. While the validity of these animal models has been
396 a source of passionate debate, empirical evidence has been most based on a sin-
397 gle example. Our polygenic approach provides a more holistic approach that is
398 urgently needed.

399 **Methods**

400 **Genotype and expression data in the training rat set**

401 The rats used for this study are part of a large multi-site project focused on ge-
402 netic analysis of complex traits (www.ratgenes.org). N/NIH heterogeneous stock
403 (HS) outbred rats are the most highly recombinant rat intercross available, and
404 are a powerful tool for genetic studies ([*Solberg Woods and Palmer, 2019*]; [*Chitre*
405 *et al., 2020*]). HS rats were created by interbreeding eight inbred strains and main-
406 tained by randomized breeding strategy to minimize inbreeding and control for
407 genetic drift.

408 For training the gene expression predictors, we used RNAseq and genotype
409 data pre-processed for *Munro et al. [2022]*. We used 88 HS male and female
410 adult rats, for which whole genome and RNA-sequencing information was avail-
411 able across five brain tissues [nucleus accumbens core (NAcc), infralimbic cortex
412 (Il), prelimbic cortex (PL), orbitofrontal cortex (OFC), and lateral habenula (Lhb);
413 Table 1]. Mean age was 85.7 ± 2.2 for males and 87.0 ± 3.8 for females. All
414 rats were group housed under standard laboratory conditions and had not been
415 through any previous experimental protocols. Genotypes were determined us-
416 ing genotyping-by-sequencing, as described previously in [*Parker et al., 2016*],
417 [*Chitre et al., 2020*] and [*Gileta et al., 2020*]. Bulk RNA-sequencing was performed
418 using Illumina HiSeq 4000 with polyA libraries, 100 bp single-end reads, and mean
419 library size of 27M. Read alignment and gene expression quantification was per-
420 formed using RSEM and counts were upper-quartile normalized, followed by ad-
421 ditional quality controlled filtering steps as described in *Munro et al. [2022]*. Gene
422 expression levels refer to transcript abundance for reads aligned to the gene's ex-
423 ons using the Ensembl Rat Transcriptome.

424 For each gene, we inverse normalized the TPM values to account for outliers
425 and fit a normal distribution. We then performed PEER factor analysis [*Stegle*
426 *et al., 2010*]. We regressed out sex, batch number, batch center and 7 PEER fac-
427 tors from the gene expression and saved the residuals for all downstream analy-
428 ses.

429 **Genotype and phenotype data in the target rat set**

430 We used genotype and phenotype data in 3,407 rats (i.e., target set) reported in
431 *Chitre et al. [2020]*. We used phenotypic information on body length (including
432 tail), BMI (including tail), body weight, fasting glucose levels, and fat pad traits (epi-
433 didymal fat, parametrial fat, and retroperitoneal fat). To simplify interpretation,
434 we aggregated the results of the three fat traits using the ACAT meta-analysis
435 method [*Liu et al., 2019*]. For each trait, sex, age, batch number and site, were
436 regressed out if they were significant and if they explained more than 2 % of the
437 variance, as described in [*Chitre et al., 2020*].

438 **Querying human gene-trait association results**

439 To retrieve analogous human gene-trait association results, we queried PhenomeX-
440 can, a web-based tool that serves gene-level association results for 4,091 traits
441 based on predicted expression in 49 GTEx tissues [Pividori *et al.*, 2020]. Ortholo-
442 gous genes (N = 22,777) were mapped with Ensembl annotation, using the *biomart*
443 R package and were one to one matched.

444 **Estimating gene expression heritability**

445 We calculated the cis-heritability of gene expression from the training set using a
446 Bayesian sparse linear mixed model, BSLMM [Zhou *et al.*, 2013], as implemented
447 in GEMMA. We used variants within the ± 1 Mb window up- and down-stream of
448 the transcription start and end of each gene annotated by Gencode v26 [Frankish
449 *et al.*, 2021]. We used the proportion of variance explained (PVE) generated by
450 GEMMA as the measure of cis-heritability of gene expression. We then display
451 only the PVE estimates of 10,268 genes that were also present in the human gene
452 expression data.

453 Heritability of human gene expression, which was also calculated with BSLMM,
454 was downloaded from the database generated by Wheeler *et al.* [2016]. Genes
455 were also limited to the same 10,268 as above.

456 **Examining polygenicity versus sparsity of gene expression**

457 To examine the polygenicity versus sparsity of gene expression in rats, we iden-
458 tified the optimal elastic net mixing parameter α , as described in Wheeler *et al.*
459 [2016]. Briefly, we compared the prediction performance of a range of elastic net
460 mixing parameters spanning from 0 to 1 (11 values from 0 to 1, with steps of 0.1).
461 If the optimal mixing parameter was closer to 0, corresponding to ridge regres-
462 sion, we deemed gene expression trait to be polygenic. In contrast, if the optimal
463 mixing parameter was closer to 1, corresponding to lasso, then the gene expres-
464 sion trait was considered to be more sparse. We also restricted the number of
465 genes in the pipeline to the 10,268 orthologous genes.

466 **Training gene expression prediction in rats**

467 To train prediction models for gene expression in rats, we used the training set
468 of 88 rats described above and followed the elastic net pipeline from predictdb.org.
469 Briefly, for each gene, we fitted an elastic net regression using the *glmnet* package
470 in R. We only included variants in the cis region (i.e., 1Mb up and downstream of
471 the transcription start and end). The regression coefficient from the best penalty
472 parameter (chosen via *glmnet*'s internal 10-fold cross validation [Zou and Hastie,
473 2005]) served as the weight for each gene. The calculated weights (w_s) are avail-
474 able in predictdb.org. For the comparison of number of predictable genes across
475 species, we ran the same cross-validated elastic net pipeline in four GTEx tissues

476 with sample sizes similar to that of the rats: Substantia Nigra, Kidney Cortex,
477 Uterus and Ovary. To ensure fair comparison, we used the same number of
478 genes that were orthologous across all four human tissues and rat tissues.

479 **Estimating overlap and enrichment of genes between rats and hu-** 480 **mans**

481 For human transcriptome prediction used in the comparison with rats, we simply
482 downloaded elastic net predictors trained in GTEx whole blood samples from
483 the PredictDB portal, as previously done in humans [Barbeira *et al.*, 2021]. This
484 model was different from the ones used in the UK Biobank for calculating the
485 PTRS weights (See Calculating PTRS in a rat target set).

486 We quantified the accuracy of the prediction models using a 10-fold cross val-
487 idated correlation (R) and correlation squared (R^2) between predicted and ob-
488 served gene expression [Zou and Hastie, 2005]. For the rat prediction models,
489 we only included genes whose prediction performance was greater than 0.01 and
490 had a non-negative correlation coefficient, as these genes were considered well
491 predicted.

492 We tested the prediction performance of our elastic net model trained in nu-
493 cleus accumbens core in an independent rat reference transcriptome set. We
494 predicted expression in the reference set of 188 individuals and compared to
495 observed genetic expression in the nucleus accumbens core.

496 **Implementing RatXcan**

497 We developed RatXcan, based on PrediXcan [Gamazon *et al.*, 2015] [Barbeira
498 *et al.*, 2018] in humans. RatXcan uses the elastic net prediction models generated
499 in the training set. In the prediction stage, we generated a predicted expression
500 matrix for all genes in the rat target set, by fitting an additive genetic model:

$$501 \quad Y_g = \sum_k w_{k,g} X_k + \epsilon$$

502 Y_g is the predicted expression of gene g , $w_{k,g}$ is the effect size of marker k for
503 gene g , X_k is the number of reference alleles of marker k and ϵ is the contribution
504 of other factors that determine the predicted gene expression, assumed to be
505 independent of the genetic component.

506 We then tested the association between the predicted expression matrix and
507 each trait; this was done for available phenotypes. We fitted a linear regression
508 of the phenotype on the predicted expression of each gene, which generated
509 gene-level association results for all gene trait pairs.

510 **Estimating overlap and enrichment of genes between rats and hu-** 511 **mans**

512 We queried PhenomeXcan to identify genes associated with analogous traits in
513 humans. PhenomeXcan provides gene level associations aggregated across all

514 available GTEx tissues, as calculated by MultiXcan (and extension of PrediXcan)
515 [Barbeira *et al.*, 2019]. To this aim, we adapted MultiXcan to similarly aggregate
516 our results across the 5 tested brain tissues in rats. We used a Q-Q plot to inspect
517 the level of enrichment across rat and human findings. To quantify enrichment,
518 we used a Mann-Whitney test as implemented in R to discern whether the distri-
519 bution of the p-values for genes in humans was the same for the genes that were
520 and were not nominally significant in rats.

521 **Calculating PTRS weights in the UK Biobank**

We calculated human-derived height and BMI PTRS weights using elastic net with a mixing parameter of 0.5, as described in Liang *et al.* [2022]. We predicted expression levels in 356,476 UK Biobank unrelated White British participants using whole blood prediction models trained in GTEx. We used the prediction models trained with UTMOST based on grouped lasso, which borrows information across tissues to improve prediction performance [Barbeira *et al.*, 2020, Hu *et al.*, 2019]. The predicted expression was generated using high quality SNPs from Hapmap2 [McCarthy *et al.*, 2016]. We performed elastic net regression with height and BMI as the predicted variables and the predicted expression matrix from 356,476 UK Biobank unrelated White British individuals. More specifically, for each regularization parameter λ , we selected weight parameters γ_g that minimized the mean squared difference between the predicted variable Y and prediction model $X\gamma + \gamma_0$ where $\hat{T}_g \in \mathbb{R}^{N \times 1}$ is the standardized predicted expression level of gene g across N individuals and $\hat{C}_l \in \mathbb{R}^{N \times 1}$ is the the observed value of the l th standardized covariate:

$$\gamma^{EN} = \underset{\gamma}{\operatorname{argmin}} \overbrace{\frac{1}{N} \|Y - X\gamma - \gamma_0\|_2^2}^{\text{loss:ly}} + \lambda\alpha \|\gamma\|_1 + \lambda_a(1 - \alpha)(\|\gamma\|_2)^2$$
$$X := [\hat{T}_1, \dots, \hat{T}_m, C_1, \dots, C_L]$$

522 where γ_0 is the intercept, m the number of genes, L is the number of covariates,
523 $\|B\|_2^2$ is the l_2 norm and the $\|B\|_1$ is the l_1 norm of the effect size vector. α de-
524 notes the elastic net mixing parameter and λ is the regularization parameter. 37
525 different λ 's were used, generating 37 different sets of predictors. Covariates in-
526 cluded age at recruitment (Data-Field 21022), sex (Data-Field 31), and the first 20
527 genetic PCs. For more details, see Liang *et al.* [2022]. The values of the regulariza-
528 tion parameters were chosen in a region likely to cover a wide range of sparsity
529 in the resulting models, from very sparse, containing a couple of genes, to dense,
530 containing all genes Liang *et al.* [2022].

531 **Calculating PTRS in a rat target set**

532 To calculate human-derived PTRS for both height and BMI in the target rats, we
533 used the predicted gene expression matrix calculated for the association stage.

534 For each rat, we multiplied the predicted expression with the corresponding weight
535 for that gene, derived from the human PTRS. The aggregated effects of these
536 weighted genes are summarized in a single score, PTRS:

$$537 \quad \text{PTRS}(\text{rat}) = \sum \gamma_g \cdot \hat{T}_g(\text{rat})$$

538 We generated 37 PTRS models for height and BMI for a range of regularization
539 parameters (Fig. 4e-f).

540 To identify biologically relevant tissues, pathways and gene sets associated
541 with the genes included in the PTRS, we applied multiple complementary analyses
542 using FUMA v1.3.8 [Watanabe *et al.*, 2017]. These included tissue enrichment
543 using differentially expressed genes across 54 specific tissue types from GTEx V8.
544 We included multiple gene sets (KEGG, Reactome, GO and Hallmark) from the
545 Molecular Signature Database (MsigDB) v7.0.

546 **Quantifying PTRS prediction performance**

547 We calculated the Pearson correlation (R) coefficient between PTRS of height and
548 BMI and analogous observed phenotypes in rats. To facilitate comparison with
549 previous papers, we report partial R^2 . In rats, we used traits that were already
550 adjusted for covariates. \tilde{R}^2 is equivalent to R^2 . We verified that using Spearman
551 correlation did not change the substance of the results (data not shown).

552 **Code and Data Availability**

553 The code used for this work is available at https://github.com/hakyimlab/Rat_Genomics_Paper_Pipeline.
554 Genotype and expression data are available through [Munro *et al.*,
555 2022]. Prediction models for gene expression in all five brain tissues in rats are
556 available at predictdb.org

557 **Acknowledgments**

558 This research has been conducted using the UK Biobank Resource under Appli-
559 cation Number 19526.

560 This work is supported by NIDA (DP1DA054394 to SSR),

561 **Author contributions**

562 A.A.P. and H.K.I. conceived the cross species PTRS and supervised the work. N.S.
563 and Y.L. performed a large portion of the analyses. N.S. and S.S-R. analyzed and
564 interpreted the results and wrote the initial draft of the manuscript. S.M., D.M.,
565 A.C., D.C., L.S-W, and O.P. pre-processed and analyzed the RNAseq, genotype,
566 and phenotype data. R.C., J.G., A.M.G., A.G., K.H., A.H., C.P.K., C.L.S-P., J.T., T.W.,
567 H.C., S.F., K.I., P.M., L.S. were involved in various aspects of the collection of the
568 rat physiological traits. All authors read, edited and approved the final version of
569 the manuscript.

570 Competing interests

571 The authors declare no conflict of interest.

572 Ethics declaration

573 Not applicable.

574 References

- 575 **Alliance ICD**, Adeyemo A, Balaconis MK, Darnes DR, Ripatti S, Widen E, Zhou A. Responsible use of polygenic risk scores in the clinic: potential benefits, risks and gaps. *Nature Medicine*. 2021; 27(11):1876–1884.
- 576
577
- 578 **Atanes P**, Ashik T, Persaud SJ. Obesity-induced changes in human islet G protein-coupled
579 receptor expression: Implications for metabolic regulation. *Pharmacology & therapeutics*. 2021; 228:107928.
- 580
- 581 **Barbeira AN**, Bonazzola R, Gamazon ER, Liang Y, Park Y, Kim-Hellmuth S, Wang G, Jiang
582 Z, Zhou D, Hormozdiari F, et al. Exploiting the GTEx resources to decipher the mechanisms at GWAS loci. *Genome biology*. 2021; 22(1):1–24.
- 583
- 584 **Barbeira AN**, Dickinson SP, Bonazzola R, Zheng J, Wheeler HE, Torres JM, Torstenson ES,
585 Shah KP, Garcia T, Edwards TL, et al. Exploring the phenotypic consequences of tissue
586 specific gene expression variation inferred from GWAS summary statistics. *Nature
587 communications*. 2018; 9(1):1–20.
- 588 **Barbeira AN**, Melia OJ, Liang Y, Bonazzola R, Wang G, Wheeler HE, Aguet F, Ardlie KG, Wen
589 X, Im HK. Fine-mapping and QTL tissue-sharing information improves the reliability of
590 causal gene identification. *Genet Epidemiol*. 2020 Sep; n/a(n/a).
- 591 **Barbeira AN**, Pividori M, Zheng J, Wheeler HE, Nicolae DL, Im HK. Integrating predicted
592 transcriptome from multiple tissues improves association detection. *PLoS genetics*.
593 2019; 15(1):e1007889.
- 594 **Chitre AS**, Polesskaya O, Holl K, Gao J, Cheng R, Bimschleger H, Garcia Martinez A, George
595 T, Gileta AF, Han W, et al. Genome-Wide Association Study in 3,173 Outbred Rats Identifies
596 Multiple Loci for Body Weight, Adiposity, and Fasting Glucose. *Obesity*. 2020;
597 28(10):1964–1973.
- 598 **Dobrindt K**, Zhang H, Das D, Abdollahi S, Prorok T, Ghosh S, Weintraub S, Genovese
599 G, Powell SK, Lund A, et al. Publicly available hiPSC lines with extreme polygenic risk
600 scores for modeling schizophrenia. *Complex psychiatry*. 2020; 6(3-4):68–82.
- 601 **Frankish A**, Diekhans M, Jungreis I, Lagarde J, Loveland JE, Mudge JM, Sisu C, Wright JC,
602 Armstrong J, Barnes I, et al. GENCODE 2021. *Nucleic acids research*. 2021; 49(D1):D916–
603 D923.
- 604 **Gamazon ER**, Wheeler HE, Shah KP, Mozaffari SV, Aquino-Michaels K, Carroll RJ, Eyster AE,
605 Denny JC, Nicolae DL, Cox NJ, et al. A gene-based association method for mapping
606 traits using reference transcriptome data. *Nature genetics*. 2015; 47(9):1091–1098.

- 607 **Gileta AF**, Gao J, Chitre AS, Bimschleger HV, St Pierre CL, Gopalakrishnan S, Palmer AA.
608 Adapting genotyping-by-sequencing and variant calling for heterogeneous stock rats.
609 *G3: Genes, Genomes, Genetics*. 2020; 10(7):2195–2205.
- 610 **Hu Y**, Li M, Lu Q, Weng H, Wang J, Zekavat SM, Yu Z, Li B, Gu J, Muchnik S, et al. A statistical
611 framework for cross-tissue transcriptome-wide association analysis. *Nature genetics*.
612 2019; 51(3):568–576.
- 613 **Huggett SB**, Johnson EC, Hatoum AS, Lai D, Srijevantham J, Bubier JA, Chesler EJ, Agrawal
614 A, Palmer AA, Edenberg HJ, et al. Genes identified in rodent studies of alcohol intake
615 are enriched for heritability of human substance use. *Alcoholism: Clinical and Exper-
616 imental Research*. 2021; .
- 617 **Lewis CM**, Vassos E. Polygenic risk scores: from research tools to clinical instruments.
618 *Genome medicine*. 2020; 12(1):1–11.
- 619 **Liang Y**, Pividori M, Manichaikul A, Palmer AA, Cox NJ, Wheeler HE, Im HK. Polygenic
620 transcriptome risk scores (PTRS) can improve portability of polygenic risk scores across
621 ancestries. *Genome Biol*. 2022 Jan; 23(1):23.
- 622 **Liu Y**, Chen S, Li Z, Morrison AC, Boerwinkle E, Lin X. ACAT: A Fast and Powerful p Value
623 Combination Method for Rare-Variant Analysis in Sequencing Studies. *Am J Hum Genet*.
624 2019 Mar; 104(3):410–421.
- 625 **Loos RJ**. 15 years of genome-wide association studies and no signs of slowing down.
626 *Nature Communications*. 2020; 11(1):1–3.
- 627 **Martin AR**, Kanai M, Kamatani Y, Okada Y, Neale BM, Daly MJ. Clinical use of current poly-
628 genic risk scores may exacerbate health disparities. *Nature genetics*. 2019; 51(4):584.
- 629 **Maurano MT**, Humbert R, Rynes E, Thurman RE, Haugen E, Wang H, Reynolds AP, Sand-
630 strom R, Qu H, Brody J, et al. Systematic localization of common disease-associated
631 variation in regulatory DNA. *Science*. 2012; 337(6099):1190–1195.
- 632 **McCarthy S**, Das S, Kretzschmar W, Delaneau O, Wood AR, Teumer A, Kang HM, Fuchs-
633 berger C, Danecek P, Sharp K, et al. A reference panel of 64,976 haplotypes for geno-
634 type imputation. *Nature genetics*. 2016; 48(10):1279.
- 635 **Mignogna KM**, Bacanu SA, Riley BP, Wolen AR, Miles MF. Cross-species alcohol
636 dependence-associated gene networks: co-analysis of mouse brain gene expression
637 and human genome-wide association data. *PLoS one*. 2019; 14(4):e0202063.
- 638 **Munro D**, , Palmer A, Mohammadi P. The regulatory landscape of multiple brain regions
639 in outbred heterogeneous stock rats. . 2022; .
- 640 **Neuner SM**, Heuer SE, Huentelman MJ, O’Connell KM, Kaczorowski CC. Harnessing ge-
641 netic complexity to enhance translatability of Alzheimer’s disease mouse models: a
642 path toward precision medicine. *Neuron*. 2019; 101(3):399–411.
- 643 **Ozawa A**, Yamada M, Satoh T, Monden T, Hashimoto K, Kohga H, Hashiba Y, Sasaki T, Mori
644 M. Transcriptional regulation of the human PRL-releasing peptide (PrRP) receptor gene

- 645 by a dopamine 2 receptor agonist: cloning and characterization of the human PrRP
646 receptor gene and its promoter region. *Molecular Endocrinology*. 2002; 16(4):785–798.
- 647 **Palmer RH**, Benca-Bachman CE, Huggett SB, Bubier JA, McGeary JE, Ramgiri N, Srijeyan-
648 than J, Yang J, Visscher PM, Yang J, et al. Multi-omic and multi-species meta-analyses
649 of nicotine consumption. *Translational psychiatry*. 2021; 11(1):1–10.
- 650 **Palmer RH**, Johnson EC, Won H, Polimanti R, Kapoor M, Chitre A, Bogue MA, Benca-
651 Bachman CE, Parker CC, Verma A, et al. Integration of evidence across human
652 and model organism studies: A meeting report. *Genes, Brain and Behavior*. 2021;
653 20(6):e12738.
- 654 **Parker CC**, Gopalakrishnan S, Carbonetto P, Gonzales NM, Leung E, Park YJ, Aryee E, Davis
655 J, Blizard DA, Ackert-Bicknell CL, et al. Genome-wide association study of behavioral,
656 physiological and gene expression traits in outbred CFW mice. *Nature genetics*. 2016;
657 48(8):919–926.
- 658 **Pividori M**, Rajagopal PS, Barbeira A, Liang Y, Melia O, Bastarache L, Park Y, Consortium
659 G, Wen X, Im HK. PhenomeXcan: Mapping the genome to the phenome through the
660 transcriptome. *Science Advances*. 2020; 6(37):eaba2083.
- 661 **Reynolds T**, Johnson EC, Huggett SB, Bubier JA, Palmer RH, Agrawal A, Baker EJ, Chesler EJ.
662 Interpretation of psychiatric genome-wide association studies with multispecies het-
663 erogeneous functional genomic data integration. *Neuropsychopharmacology*. 2021;
664 46(1):86–97.
- 665 **Saeed S**, Bonnefond A, Tamanini F, Mirza MU, Manzoor J, Janjua QM, Din SM, Gaitan J,
666 Milochau A, Durand E, et al. Loss-of-function mutations in ADCY3 cause monogenic
667 severe obesity. *Nature genetics*. 2018; 50(2):175–179.
- 668 **So HC**, Chau CKL, Chiu WT, Ho KS, Lo CP, Yim SHY, Sham PC. Analysis of genome-wide
669 association data highlights candidates for drug repositioning in psychiatry. *Nature*
670 *neuroscience*. 2017; 20(10):1342–1349.
- 671 **Solberg Woods LC**, Palmer AA. Using heterogeneous stocks for fine-mapping genetically
672 complex traits. *Rat genomics*. 2019; p. 233–247.
- 673 **Speliotes EK**, Willer CJ, Berndt SI, Monda KL, Thorleifsson G, Jackson AU, Allen HL, Lind-
674 gren CM, Luan J, Mägi R, Randall JC, Vedantam S, Winkler TW, Qi L, Workalemahu T,
675 Heid IM, Steinthorsdottir V, Stringham HM, Weedon MN, Wheeler E, et al. Association
676 analyses of 249,796 individuals reveal 18 new loci associated with body mass index.
677 *Nat Genet*. 2010 Oct; 42(11):937–948.
- 678 **Stegle O**, Parts L, Durbin R, Winn J. A Bayesian framework to account for complex non-
679 genetic factors in gene expression levels greatly increases power in eQTL studies. *PLoS*
680 *computational biology*. 2010; 6(5):e1000770.
- 681 **Visscher PM**, Wray NR, Zhang Q, Sklar P, McCarthy MI, Brown MA, Yang J. 10 years of
682 GWAS discovery: biology, function, and translation. *The American Journal of Human*
683 *Genetics*. 2017; 101(1):5–22.

- 684 **Watanabe K**, Taskesen E, Van Bochoven A, Posthuma D. Functional mapping and anno-
685 tation of genetic associations with FUMA. *Nature communications*. 2017; 8(1):1–11.
- 686 **Wheeler HE**, Shah KP, Brenner J, Garcia T, Aquino-Michaels K, Consortium G, Cox NJ,
687 Nicolae DL, Im HK. Survey of the heritability and sparse architecture of gene expression
688 traits across human tissues. *PLoS genetics*. 2016; 12(11):e1006423.
- 689 **Wood AR**, Esko T, Yang J, Vedantam S, Pers TH, Gustafsson S, Chu AY, Estrada K, Kutalik
690 Z, Amin N, et al. Defining the role of common variation in the genomic and biological
691 architecture of adult human height. *Nature genetics*. 2014; 46(11):1173–1186.
- 692 **Wray NR**, Goddard ME, Visscher PM. Prediction of individual genetic risk to disease from
693 genome-wide association studies. *Genome research*. 2007; 17(10):1520–1528.
- 694 **Yengo L**, Sidorenko J, Kemper KE, Zheng Z, Wood AR, Weedon MN, Frayling TM,
695 Hirschhorn J, Yang J, Visscher PM, et al. Meta-analysis of genome-wide association
696 studies for height and body mass index in 700000 individuals of European ancestry.
697 *Human molecular genetics*. 2018; 27(20):3641–3649.
- 698 **Zhao X**, Gu J, Li M, Xi J, Sun W, Song G, Liu G. Pathway analysis of body mass index genome-
699 wide association study highlights risk pathways in cardiovascular disease. *Scientific*
700 *reports*. 2015; 5(1):1–7.
- 701 **Zhou X**, Carbonetto P, Stephens M. Polygenic modeling with bayesian sparse linear
702 mixed models. *PLoS Genet*. 2013 Feb; 9(2):e1003264–e1003264.
- 703 **Zou H**, Hastie T. Regularization and variable selection via the elastic net. *Journal of the*
704 *royal statistical society: series B (statistical methodology)*. 2005; 67(2):301–320.

705 **Supplementary information**

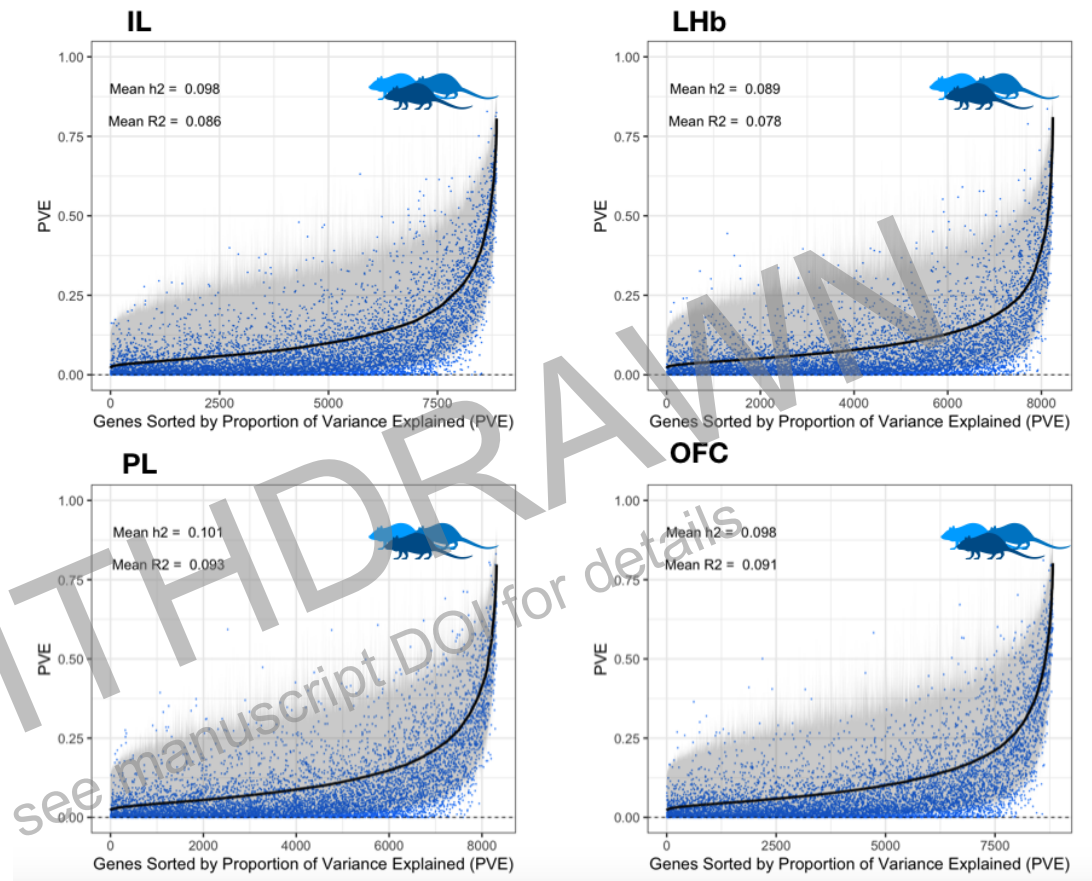


Figure S1. Gene expression was heritable [8.86-10.12%] and comparable across several brain tissues tested (Infralimbic Cortex, IL; Lateral Habenula, LHB; Prelimbic Cortex, PL; Orbitofrontal Cortex, OFC) in rats. We refer to heritability (h^2 , cis-heritability within 1Mb) as the proportion of variance explained (PVE). Across all brain tissues tested, heritability estimates were significantly correlated ($R = [0.58 - 0.83]$, $P < 2.20 \times 10^{-16}$).

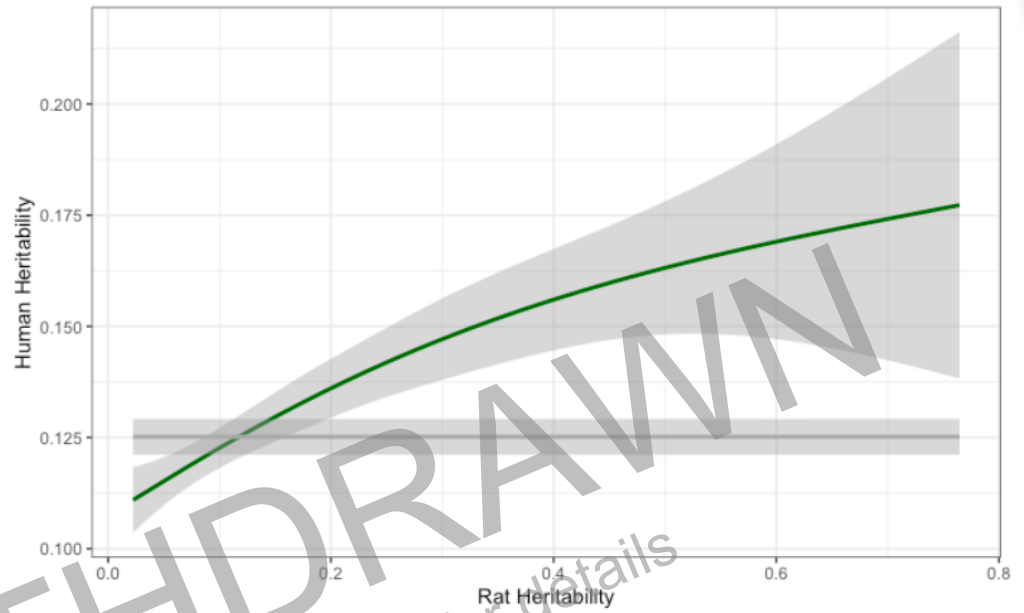


Figure S2. Heritability of gene expression was correlated between rats and humans. We found a significant correlation ($R = 0.067$, $P = 4.34 \times 10^{-12}$) between heritability estimates in rats and humans. Confidence intervals are represented as gray bars. The gray line represents the null distribution.

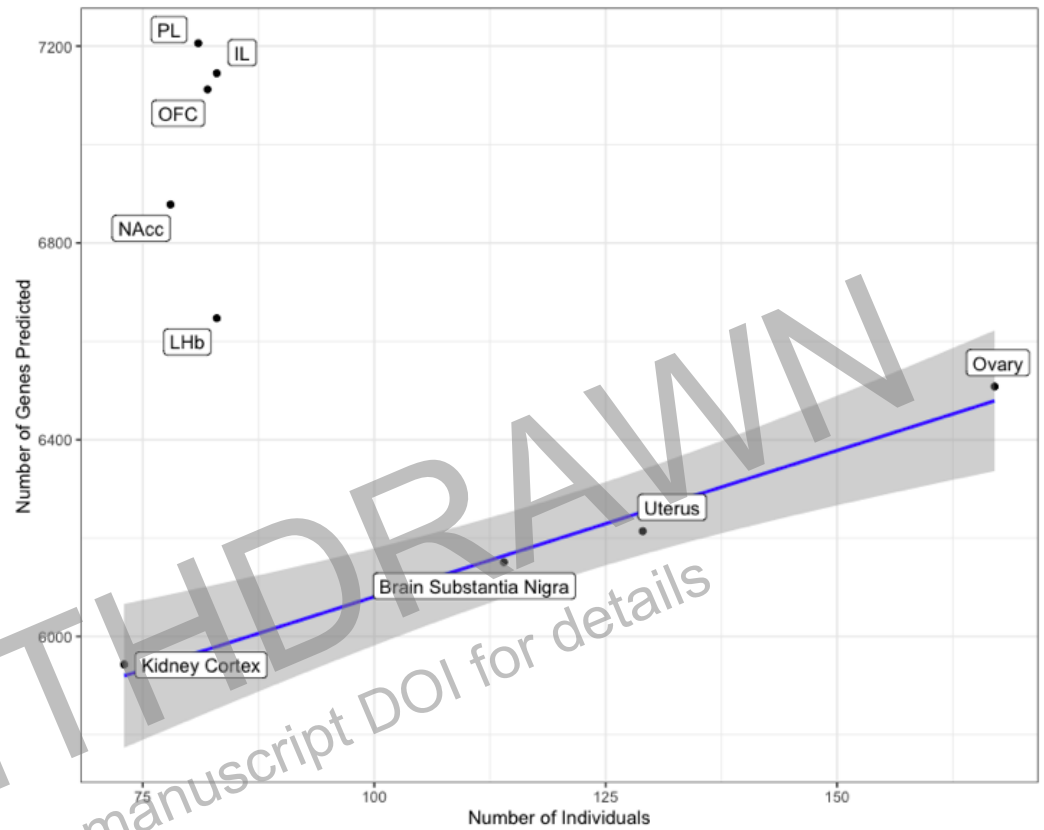


Figure S3. Prediction was greater in rat tissues than that in human GTEx tissues.

The number of predicted genes across all five rat tissues was greater than those in GTEx human tissues with similar sample size. To ensure fair comparison, we included the same subset of genes that were orthologous across all tested tissues.

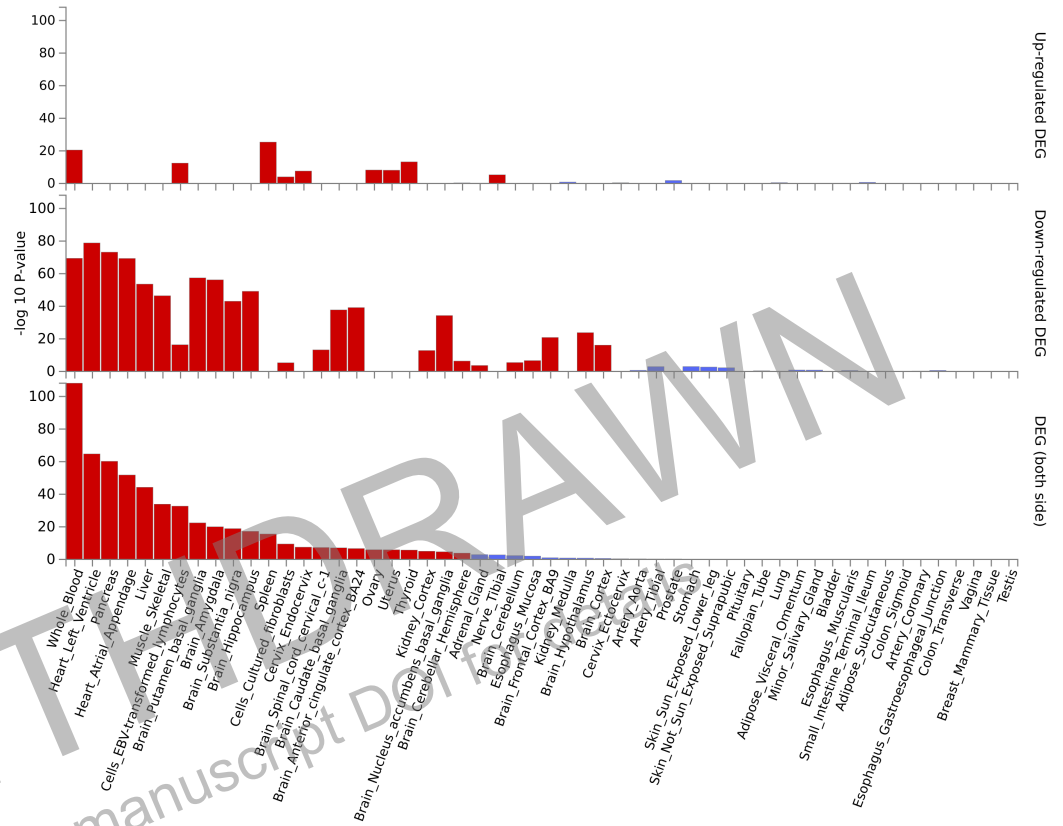


Figure S4. Tissue analysis revealed substantial enrichment in multiple relevant tissues, including heart, pancreas, muscle, liver, and central nervous system. Significantly enriched sets ($P < 0.05$) are highlighted in red.

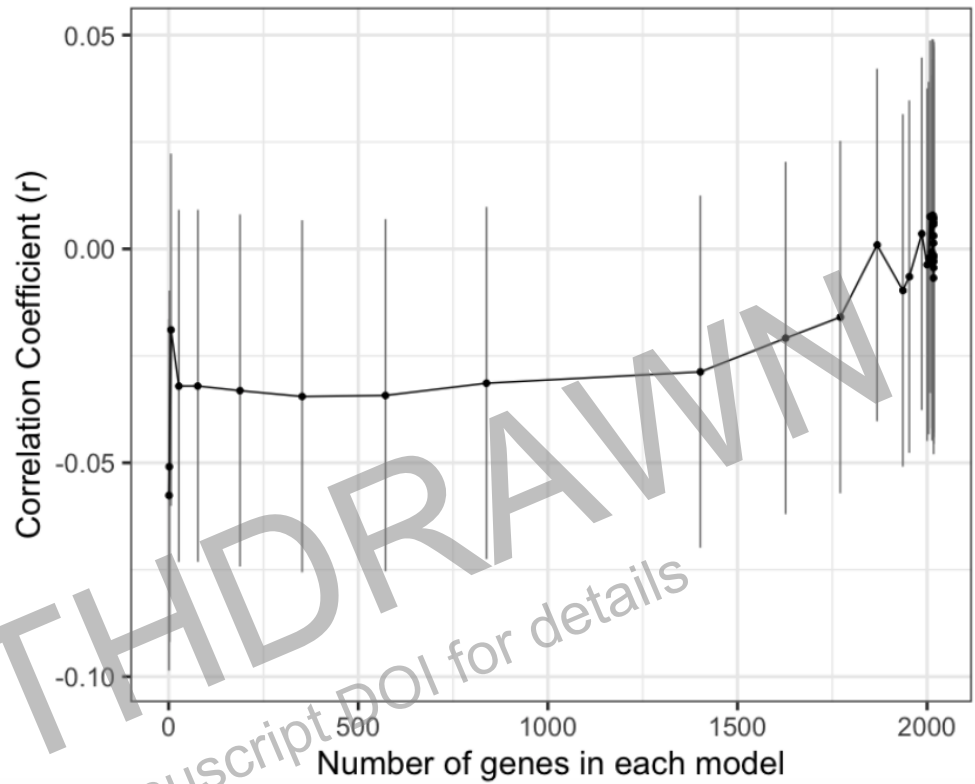


Figure S5. Human derived PTRS weights did not predict observed fasting glucose levels in rats. Human-derived height PTRS in rats was not correlated with observed fasting glucose levels in the target rat set ($R = 0.008$, $P = 7.09 \times 10^{-1}$), which served as a negative control.